Rare Met. (2018) 37(1):66–71
https://doi.org/10.1007/s12598-015-0552-z

RARE METALS
www.editorialmanager.com/rmet

Phase transformation of ZrO_2 doped with CeO_2

Bo He, Ying Li, Hong-Yu Zhang, Duo-Li Wu, Li-Hong Liang, Hua Wei*

Received: 19 June 2014 / Revised: 29 June 2014 / Accepted: 23 June 2015 / Published online: 23 July 2015

Abstract Thermal barrier coatings (TBCs) protection is widely used to prolong the lifetime of turbine components. The outermost layer of TBCs is ceramic layer, whose function is heat insulation, and the main composition of the ceramic layer is ZrO_2. In this study, the micro-ZrO_2 and the nano-ZrO_2 doped with 10 wt% CeO_2 as well as micro-ZrO_2 and nano-ZrO_2 were prepared by air plasma spraying (APS) to study the advantages of the addition of rare earth element. The effect of CeO_2 on the phase transformation of ZrO_2 was studied. The results show that there are few cracks in micro- and nano-ZrO_2 doped with 10 wt% CeO_2, and rare earth oxides can affect the phase transformation significantly. The morphologies, hardness and elastic modulus of the four ceramic layers were also discussed.

Keywords Ceramic layer; Rare earth oxides; Phase transformation; CeO_2

1 Introduction

Thermal barrier coating (TBC) is a multilayer material applied to the surface of the high-temperature alloy, playing a key role in protecting the metallic materials [1]. TBCs have a wide application on aviation turbine engine blades, whose major functions are heat insulation, oxidation resistance and corrosion resistance [2, 3]. It is composed of three layers, i.e., a ceramic layer, an oxide layer and a metal bonding layer, one following another. The bonding layer is directly contacted with the substrate, and the commonly used material is MCrAlY, whose purpose is to provide better integration of the ceramic layer and the substrate. As ceramic layer is an oxygen ion conductor under high temperature, it also takes the role of oxidation resistance [4]. The metal oxide layer is resulted from the oxidation of the metal bonding layer under high temperature, whose main component is Al_2O_3, taking the role of oxidant resistance, but it also affects the life of thermal barrier coatings [5, 6]. The outermost layer of the thermal barrier coatings is the ceramic layer, whose main function is heat insulation and reducing the operating temperature of the substrate.

The main component of ceramic layer is ZrO_2, and the pure powder of ZrO_2 at a normal temperature environment is monoclinic phase [7], having a high melting point and chemical inertness. However, monoclinic ZrO_2 is easily corroded, and in the process of phase transformation from monoclinic phase to tetragonal phase, volume expansion from 5 % to 8 % will be generated, which leads to the cracking of coatings. Therefore, some stabilizers, such as Y_2O_3, should be added for the purpose of replacing monoclinic phase with tetragonal phase of ZrO_2 and improving its chemical stability. Although the ceramic layer has good wear resistance and heat insulation, it also has high brittleness and low shock resistance, which is the key factor for crack initiation. In order to exploit the potentiality of zirconium ceramic layer, nanometer-level yttria-stabilized zirconia (YSZ) powder was used. It has higher hardness,

B. He, Y. Li
School of Mechatronics Engineering, Shenyang Aerospace University, Shenyang 110136, China

Y. Li, H.-Y. Zhang, D.-L. Wu, H. Wei*
Institute of Metal Research, Chinese Academy of Sciences, Shenyang 110016, China
e-mail: hwei@imr.ac.cn

L.-H. Liang
Institute of Mechanics, Chinese Academy of Sciences, Beijing 100190, China

better heat insulation effect and wear resistance than microceramic layer prepared by air plasma spraying (APS). The principle is that the nanometer thermal barrier coatings by APS have partially melting nanocrystal material YSZ particles, which can play a role in improving the coating performance. The toughness and heat transfer of the coatings are improved due to the dispersion strength of nanocrystal particle. Compared with the conventional APS coatings, its microhardness and spalling resistance performance are improved significantly.

With the development of aviation technology and the increase in thrust–weight ratio of turbine blades, TBCs' operating temperature becomes higher and higher, and the existing Y_2O_3 cannot fully ensure the stability of the YSZ. Studies found that rare earth elements can improve the stability, toughness and shock resistance of ceramic layer [8]. About new thermal barrier coating materials, most researches focus on stabilizer of YSZ material and compound ceramic material. Nicholls et al. [9] found that the addition of rare earth oxide elements can reduce the thermal conductivity of the thermal barrier coating. For example, YSZ added CeO_2 cannot only reduce the thermal conductivity, but also improve its fracture toughness; although the thermal conductivity of YSZ added La_2O_3 reduces distinguishably, its thermal fatigue life decreases with the increase in La_2O_3 content [10, 11]. Matsumotoa et al. [12] found that it can inhibit sintering of YSZ in electron beam physical vapor deposition (EB-PVD) process if a small amount of La_2O_3 was added. At the same time, it can form feathery crystalline structure and nanometer pores which can help decrease thermal conductivity. Nd_2O_3 mixed with Sm_2O_3 and Sc_2O_3 can also reduce the thermal conductivity of TBCs [13, 14]. Vassen et al. proved that $La_2Zr_2O_7$ have high melting point and low thermal conductivity, but its low expansion leads to poor thermal shock resistance [15]. The thermal conductivity of $Nd_2Ce_2O_7$ is less than that of 8YSZ, but its coefficient thermal expansion is higher [16, 17].

Most of the studies concerned rare earth element only on one-sidedness performance of thermal barrier coatings, which is not perfectly expounded on whole performance of the thermal barrier coatings. Therefore, in this study, the micro-ZrO_2 and the nano-ZrO_2 doped with 10 wt% CeO_2 were in contrast with the normal micro-ZrO_2 and the nano-ZrO_2 to show the superiority of the formers and study the whole performance of the thermal barrier coatings.

2 Experimental

2.1 Manufacture of TBCs

The thermal barrier coatings were prepared by APS. Before spraying, the matrix alloy was treated by acetone and abrasion blasting to obtain a better combination with the ceramic thermal barrier coatings (TBCs). Firstly, the matrix alloy was interposed into a special chucking appliance. And then the matrix alloy should be preheated to the temperature of achieving the spraying process. And spraying parameters should be determined properly to ensure the nanometer power to keep a surface melting and internal non-melting condition that could make a strong bond in the nano-ZrO_2 particles. Spraying distance was preferably maintained between 80 and 120 mm, and the paint spraying gun should be perpendicular to the surface of the matrix for spraying as possible as it could.

2.2 Characterization of morphology and hardness

Ni-based superalloy with nominal composition of 8.39 wt% Cr, 5.01 wt% Co, 9.47 wt% W, 5.47 wt% Y, 2.14 wt% Ti, 2.92 wt% Ta, and balanced Ni was used as substrate. Microstructure and morphology were characterized by scanning electronic microscope (SEM). Gold spraying was done to the sample before scanning, which is beneficial to conductivity.

Four work pieces coated with normal nano-ZrO_2, micro-ZrO_2, micro-ZrO_2 doped with 10 wt% CeO_2 and nano-ZrO_2 doped with 10 wt% CeO_2 were divided into a group, seven groups were prepared totally, six of them were, respectively placed in a constant temperature furnace of 1000, 1050, 1100, 1150, 1200, 1250 °C, and the seventh was stored at room temperature. The coatings in the constant temperature furnaces were heated under the high temperature for 200 h and then removed to air for cooling. In order to detect the ceramic layer phase, the four work pieces coated with normal nano-ZrO_2, the micro-ZrO_2, the 10 wt% CeO_2-doped micro-ZrO_2 and the 10 wt% CeO_2-doped nano-ZrO_2 were detected by DX-2000 X-ray diffractometer (XRD) for phase identification of the ceramic layer after APS.

U9830A agilent G300 nano-indentation apparatus was used to do the nano-indentation experiment to measure the microscopic hardness and elastic modulus of the samples. Samples were sanded and polished before measurement to make the surface smooth and get more accurate data.

3 Results and discussion

3.1 Surface and cross-sectional morphologies of TBCs

Figure 1a–d shows the surface morphologies of nano-ZrO_2, micro-ZrO_2, nano-ZrO_2 doped with 10 wt% CeO_2 and micro-ZrO_2 doped with 10 wt% CeO_2, respectively, at normal temperature. The four kinds of the ceramic coatings are completely melted. As the ceramic coating rested a

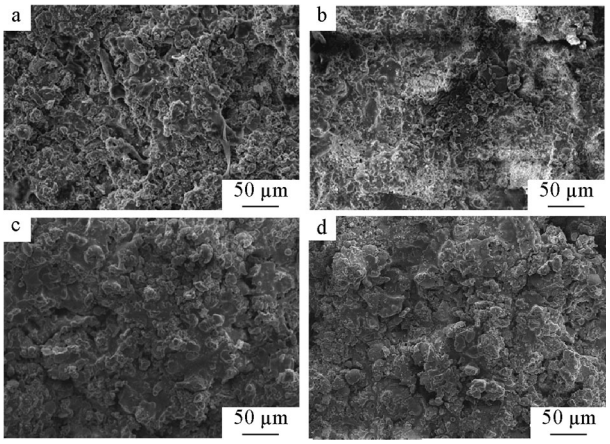

Fig. 1 SEM images of coatings surfaces: **a** nano-ZrO_2, **b** micro-ZrO_2, **c** nano-ZrO_2 doped with 10 wt% CeO_2, and **d** micro-ZrO_2 doped with 10 wt% CeO_2

very short time in the ion jet before impacted to the substrate, and then cooled down rapidly in static air, it has a good flatting appearance comparatively. The four coating surfaces are relatively smooth and compact with few microscopic cracks, and better surface uniformities of the nano-ZrO_2, the nano-ZrO_2 doped with 10 wt% CeO_2 and micro-ZrO_2 doped with 10 wt% CeO_2 are obtained.

Figure 2 shows the surface morphologies of the four coatings after oxidation at 1000 °C for 120 h. No cracking and spallation appear, and the oxidation resistances of the four coatings are good. From the morphologies, it can be seen that no phase and recombinant are observed. However, during the oxidation process, some small oxidation particles generate because ceramic is oxidized in micro-ZrO_2 and nano-ZrO_2, making the topography surface become rough, while micro-ZrO_2 doped with 10 wt% CeO_2 and nano-ZrO_2 doped with 10 wt% CeO_2 maintain lamellar structure obviously.

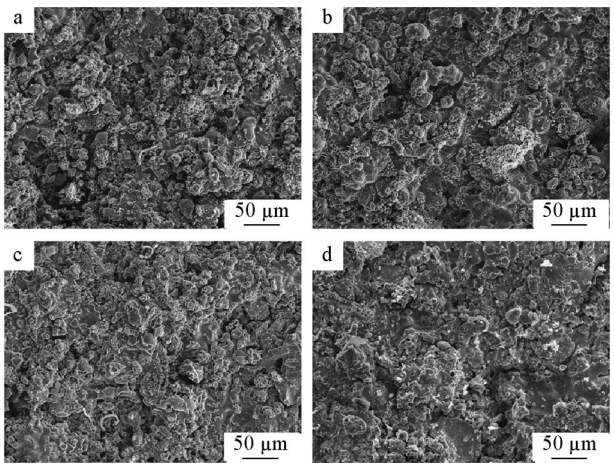

Fig. 2 SEM images of coating surfaces at 1000 °C for 120 h: **a** nano-ZrO_2, **b** micro-ZrO_2, **c** nano-ZrO_2 doped with 10 wt% CeO_2, and **d** micro-ZrO_2 doped with 10 wt% CeO_2

Figure 3 shows the sectional morphologies of the four coatings, and the samples were ground and polished after being cut and mounted. It can be observed that the surfaces of micro-ZrO_2 doped with 10 wt% CeO_2 and nano-ZrO_2 doped with 10 wt% CeO_2 are smoother than those of micro-ZrO_2 and nano-ZrO_2. There are not large pores between the metal bonding layer and the ceramic layer along with less cracks in it. Most of the cracks are longitudinal cracks, which can alleviate thermal stress and inhibit the initiation and growth of the horizontal crack, improving the thermal shock lifetime of coatings. There are some horizontal cracks existing in nano-ZrO_2 and micro-ZrO_2. Horizontal crack can lead to the destruction of the coatings, reducing the thermal shock lifetime of the TBCs.

3.2 Phase content proportion of ceramic layer

At room temperature, the pure ZrO_2 is monoclinic. And it will transform into tetragonal phase after being heated under the temperature of about 1200 °C with the volume shrinkage of 5 %. And if the temperature is further higher, cubic phase will be produced. In the cooling process, the transformation temperature of tetragonal phase to monoclinic phase is about 1000 °C, and there is a volume bulking of 8 %. This is called the thermal hysteresis phenomenon which commonly occurs in polycrystalline transformation and can lead to the thermal barrier coatings cracking [18]. And Y^{3+} can displace Zr^{4+} and react with oxygen atoms, so that the phase transformation of ZrO_2 is prevented from tetragonal to monoclinic phase. Thus, the stabilizer is added into ZrO_2 so that the transformation temperature from tetragonal phase to the monoclinic phase can be reduced to room temperature [19]. And it is the stress induction that makes the transformation temperature change from tetragonal phase to monoclinic phase down to

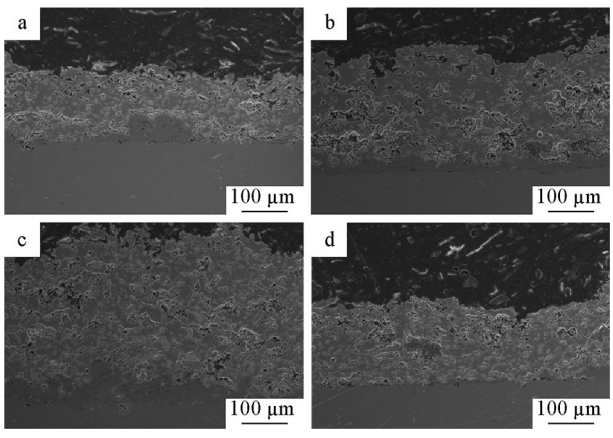

Fig. 3 Sectional SEM images of thermal barrier coatings: **a** nano-ZrO_2, **b** micro-ZrO_2, **c** nano-ZrO_2 doped with 10 wt% CeO_2, and **d** micro-ZrO_2 doped with 10 wt% CeO_2

room temperature, which leads to the transformation toughening phenomenon. Among the tetragonal phase, monoclinic phase and the cubic phase, the cubic phase has the most stable quality undoubtedly. Therefore, efforts should be made to avoid the monoclinic phase and at the same time make the cubic phase account for a larger proportion, which can improve the thermal stability of coatings. In order to make the monoclinic phase reduce or even disappear, rare earth oxides were added into ceria-stabilized ZrO_2 ceramics. At the same time, the cubic phase content increases, which could produce a more stable ceramic coating.

Figure 4 shows the phase structure comparisons of the coatings of four components at the same temperature. All of the curves were acquired by MDI Jade 6.

The analyses of XRD patterns show that between 1000 and 1250 °C, the normal nano-ZrO_2, micro-ZrO_2, micro-ZrO_2 doped with 10 wt% CeO_2 and nano-ZrO_2 doped with 10 wt% CeO_2 are all tetragonal and cubic. At 1250 °C, there are a small amount of monoclinic phases appearing in micro-ZrO_2 coating and nano-ZrO_2 coating. By the following formula, the content of the monoclinic phase and the tetragonal phase can be calculated [20].

$$I_1/I_2 = \mathrm{RIR}_1 \cdot \omega_1/\mathrm{RIR}_2 \cdot \omega_2 \quad (1)$$

where I_1 and I_2 are the strongest peak areas of monoclinic phase and tetragonal phase, respectively; RIR_1 and RIR_2 are the intensity ratios of monoclinic phase and tetragonal phase when the phase content is the same with the standard phase content, respectively; ω_1 and ω_2 are the phase mass ratios of monoclinic ZrO_2 and tetragonal ZrO_2, respectively. From the formula, at 1250 °C, the phase mass ratio of nano-ZrO_2 monoclinic phase and tetragonal phase is 9.75 %, and the phase mass ratio of micro-ZrO_2 monoclinic and tetragonal is 13.25 %. It proves that, under the same conditions, nano-sized coating has a better structure and phase stability than the micro-sized coating. There is no monoclinic phase existing in nano-ZrO_2 doped with 10 % CeO_2 and micro-ZrO_2 doped with 10 wt% CeO_2, indicating that the rare earth oxides affect the phase transformation remarkably.

As the index of crystallographic orientation of the cubic phase in one direction accords with that of tetragonal phase and the crystal structures of them are very similar, Eq. (1) cannot be used to calculate the phase mass ratio of nano-ZrO_2 tetragonal phase and cubic phase. Because the phase content is proportional to the phase of the diffraction intensity, the contents of cubic phase can be compared by the corresponding diffraction peak intensity and the diffraction area. Table 1 shows the four diffraction peak areas of the coatings under different temperatures. Area value was acquired by MDI Jade 6, and big area value indicates that the cubic phase is stronger.

Overall, the strength of the cubic phase of CeO_2-doped coating is higher than that of the coating without rare earth elements, and there is not any monoclinic phase at all, because the formation of ionic substitution solid solution mainly leads to the good organizational stability of the tetragonal phase under room temperature. The radius of Ce^{4+} is close to that of Zr^{4+}, so it is easy to replace Zr^{4+} with ZrO_2, leading to weak lattice distortion and hindering the phase transformation of t-ZrO_2 to m-ZrO_2 during cooling lattice twist process. Finally, the tetragonal phase can be preserved in the metastable manner at low temperatures [21].

3.3 Hardness and elastic modulus of coatings

Higher hardness means better wear resistance. The smaller the friction coefficient is, the better the abrasion resistance is. The results of Table 2 show that the hardness of nano-ZrO_2 doped with 10 wt% CeO_2 and micro-ZrO_2 doped with 10 wt% CeO_2 is smaller than that of nano-ZrO_2 and micro-ZrO_2 at room temperature, but the hardness of nano-ZrO_2 doped with 10 wt% CeO_2 and micro-ZrO_2 doped

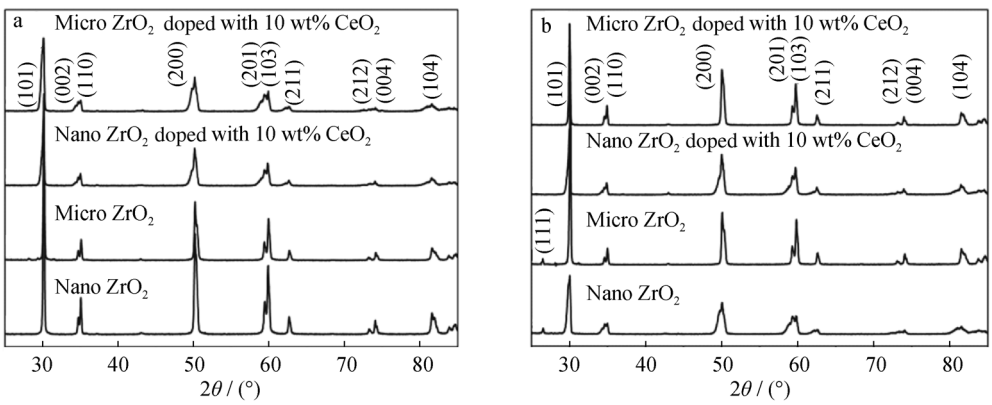

Fig. 4 XRD patterns of illustrative plates of coatings at **a** 1200 and **b** 1250 °C

Table 1 Areas of four coatings at different temperatures (cps)

Coatings	Normal	1000 °C	1050 °C	1100 °C	1150 °C	1200 °C	1250 °C
Nano ZrO_2	109,436	51,376	116,387	19,332	14,816	67,891	70,910
Micro ZrO_2	105,194	47,119	66,683	64,577	47,530	67,032	20,763
Nano ZrO_2 doped with 10 wt% CeO_2	136,663	51,336	62,543	68,349	35,983	93,596	79,372
Micro ZrO_2 doped with 10 wt% CeO_2	130,360	61,453	72,627	77,979	40,956	92,158	77,264

Table 2 Hardness of four coatings under room temperature and 1000 °C (GPa)

Coatings	Nano ZrO_2	Micro ZrO_2	Nano ZrO_2 doped with 10 wt% CeO_2	Micro ZrO_2 doped with 10 wt% CeO_2
Normal	11.206	11.559	9.197	8.636
1000 °C	11.528	11.895	12.959	13.019

Table 3 Elastic modulus of four coatings under room temperature and 1000 °C (GPa)

Coatings	Nano ZrO_2	Micro ZrO_2	Nano ZrO_2 doped with 10 wt% CeO_2	Micro ZrO_2 doped with 10 wt% CeO_2
Normal	128.266	126.311	113.719	129.719
1000 °C	153.395	147.146	162.332	158.098

with 10 wt% CeO_2 at operating temperature rises faster than that of nanometer ZrO_2 and micro-ZrO_2. But the coating quality should be valuated at operating temperature; therefore, the coating doped with rare earth oxide has better abrasion resistance.

A number of factors associated with the thermal barrier coating spalling failure are related to the elastic modulus, so the elastic modulus is also one of the important parameters to evaluate the performance of thermal barrier coatings. The larger the elastic modulus is, the larger the strength with the atoms is, and so when the elastic modulus is larger, the tensile strength of coating will be relatively larger. From the experimental data (Table 3), the elastic modulus of four kinds of coatings does not have too many differences, so the addition of rare earth elements does not affect the tensile strength of coatings.

4 Conclusion

In this paper, the superiority of rare earth-doped ZrO_2 was confirmed based on experiments. At room temperature, the four coating surfaces are relatively smooth and compact, there are few microscopic cracks, and the better surface uniformities of the nano-ZrO_2 powders and micro-ZrO_2 powders doped with 10 wt% CeO_2 are obtained. After heating for 120 h under 1000 °C, the surfaces of nano-ZrO_2 powders and micro-ZrO_2 powders doped with 10 wt% CeO_2 are smoother than those of the nano-ZrO_2 powders and micro-ZrO_2 powders. According to the cross section, there are few cracks in micro- and nano-ZrO_2 doped with 10 wt% CeO_2, and the cracks are mostly longitudinal cracks. At the temperatures of 1000 and 1200 °C, there are only tetragonal phases and cubic phases in the four coatings. At 1250 °C, there are a small amount of monoclinic phases appearing in the micro- and nano-ZrO_2 coatings, but there is no monoclinic phase in nano-ZrO_2 and micro-ZrO_2 doped with 10 wt% cerium oxide. And the strength of cubic phase of the coating doped with CeO_2 is higher than that of the coating without rare earth elements. In nano-indentation experiments, hardness of coating doped with rare earth oxide at operating temperature is higher than that of normal micro- and nano-ZrO_2, so the coating doped with rare earth oxide has better abrasion resistance. The elastic moduli of the four kinds of coatings do not have much difference, so the addition of rare earth elements does not affect the tensile strengths of coatings.

Acknowledgments This study was financially supported by the National Natural Science Foundation of China (No. 51371173), the Natural Science Foundation of Liaoning Province (No. 2013024011) and the Doctor Start-Up Fund of Liaoning Province (No. 20121063).

References

[1] Zhou YCH, Liu XQ, Li Y, Wu DJ, Mao WG. Failure mechanisms and life prediction of thermal barrier coatings. J Solid Mech. 2010;31(5):504.

[2] Zhong XH, Zhao HY, Zhou XM, Liu CG, Wang L, Shao F, Yang K, Tao SY, Ding CX. Thermal shock behavior of toughened gadolinium zirconate/YSZ double-ceramic-layered thermal barrier coating. J Alloys Compd. 2014;593(25):50.

[3] Naga SM. Ceramic matrix composite thermal barrier coatings for turbine parts. Adv Ceram Matrix Compos. 2014;. doi:10.1533/9780857098825.3.524.

[4] Su L, Wu HC, Lei XG, Liu L. Failure analysis on TBCs with thin bond coating in EB-PVD process. Mater Heat Treat. 2011;40(24):243.

[5] Hao YF, Tang WJ, Wang HY, Chen H. The analysis of the organizational structure and thermal shock performance of the nano zirconia structure thermal barrier coating. Weld Technol. 2010;31(3):109.

[6] Chen ZB, Wang ZG, Zhu SJ. Failure behavior of thermal barrier coatings on cylindrical superalloy tube was investigated under thermomechanical fatigue. Acta Metall Sin. 2013;26(4):404.

[7] Li MH, Sun XF, Zhang CY, Hu WY, Guan HG, Hu ZL. Structure and morphology changes of Al_2O_3 membrane by the oxidation of spring NiCrAlY. Corros Sci Prot Technol. 2010;31(3):142.

[8] Liu RX, Guo F, Li PF, Liu L, Wang S, Zhao RR, Zhang YL. Effect of RE element in magnesium alloy on surface morphology and structure of ceramic coating by micro-arc oxidation. Heat Treat Met. 2008;33(11):70.

[9] Nicholls JR, Lawson KJ, Johnstone A, Rickerby DS. Methods to reduce the thermal conductivity of EB-PVD TBCs. Surf Coat Technol. 2002;151–152:383.

[10] Masayuki ARAI. Inelastic constitutive equation of plasma-sprayed ceramic thermal barrier coatings. Acta Metall Sin (Engl Lett). 2011;24(2):161.

[11] Dai H, Zhong X, Li J, Zhang Y, Meng J, Cao X. Thermal stability of double-ceramic-layer thermal barrier coatings with various coating thickness. Mater Sci Eng A. 2006;433(1–2):1.

[12] Matsumotoa M, Aoyama K, Matsubar H. Thermal conductivity and phase stability of plasma sprayed ZrO_2–Y_2O_3–La_2O_3 coatings. Surf Coat Technol. 2005;194(1):31.

[13] Matsumoto M, Yamaguchi N, Matsubara H. Low thermal conductivity and high temperature stability of ZrO_2–Y_2O_3–La_2O_3 coatings produced by electron beam PVD. Scr Mater. 2004;50(6):867.

[14] Chen D, Chu ZM, Zhang Q. Analysis of several test methods about heat insulation capabilities of ceramic thermal barrier coatings. Phys Procedia. 2013;50:248.

[15] Cao XQ, Vassen R, Tietz F, Stoever D. New double-Ceramic-layer thermal barrier coatings based on zirconia-rare earth composite oxides. J Eur Ceram Soc. 2006;26(3):247.

[16] Dai H, Zhong XH, Li JY, Meng J, Cao XQ. Neodymium–cerium oxide as new thermal barrier coating material. Surf Coat Technol. 2006;201(6):2527.

[17] Zhong XH, Xu ZH, Zhang YF, Zhang JF, Cao XQ. Phase stability and thermophysical properties of neodymium cerium composite oxide. J Alloys Compd. 2009;469(1–2):82.

[18] Bahadori E, Javadpour S, Shariat MH, Mahzoon F. Preparation and properties of ceramic Al_2O_3 coating as TBCs on MCrAlY layer applied on Inconel alloy by cathodic plasma electrolytic deposition. Surf Coat Technol. 2013;228(1):S611.

[19] Han M, Huang JH, Chen SH. Behavior and mechanism of the stress buffer effect of the inside ceramic layer to the top ceramic layer in a double-ceramic-layer thermal barrier coating. Ceram Int. 2014;40(2):2901.

[20] Chen YX, Liang XB, Bai JY, Xu BS. High velocity electric arc sprayed Fe–Al–Nb–B composite coating and its wear behavior. Acta Metall Sin (Engl Lett). 2011;26(3):313.

[21] Richer P, Zuniga A, Yandouzi M, Jodoin B. CoNiCrAlY microstructural changes induced during cold gas dynamic spraying. Surf Coat Technol. 2008;203(3–4):364.